Figure S1

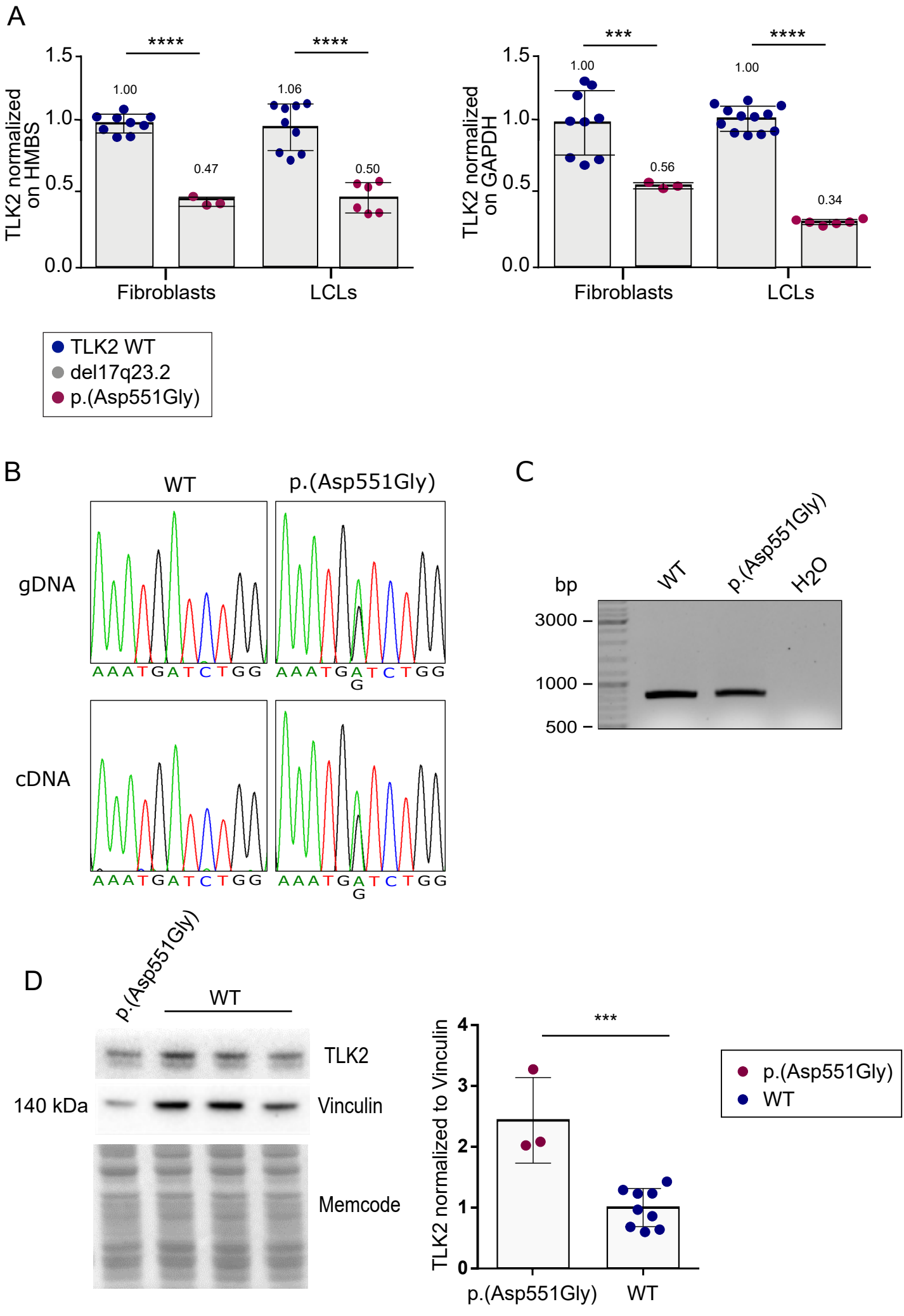
A
TLK2 normalized on HMBS
1.5
1.0
0.5
0.0
****
****
1.00
0.47
1.06
0.50
Fibroblasts
LCLs
TLK2 normalized on GAPDH
***
****
1.00
0.56
1.00
0.34
Fibroblasts
LCLs
TLK2 WT
del17q23.2
p.(Asp551Gly)
B
WT
p.(Asp551Gly)
gDNA
cDNA
AAATGATCTGG
AAATGATCTGG
G
C
bp
WT
p.(Asp551Gly)
H2O
3000
1000
500
D
p.(Asp551Gly)
WT
140 kDa
TLK2
Vinculin
Memcode
TLK2 normalized to Vinculin
***
p.(Asp551Gly)
WT

Figure S2

A

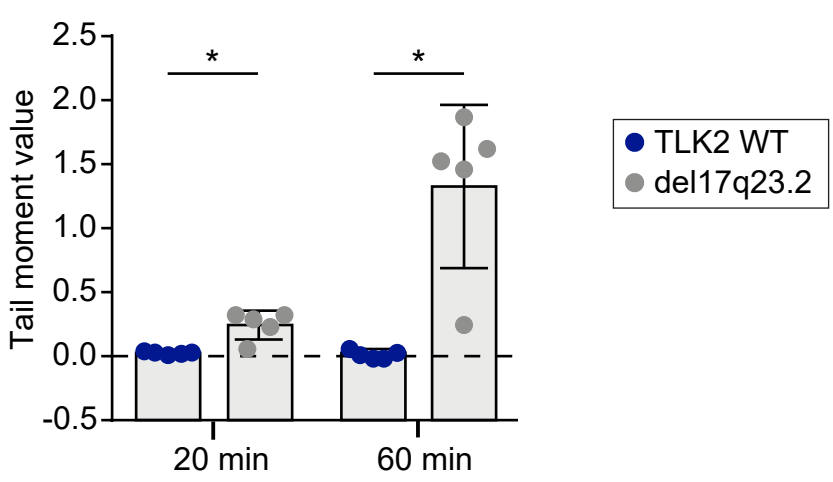
Tail moment value
2.5
2.0
1.5
1.0
0.5
0.0
-0.5
*
*
20 min
60 min
TLK2 WT
del17q23.2

Figure S3

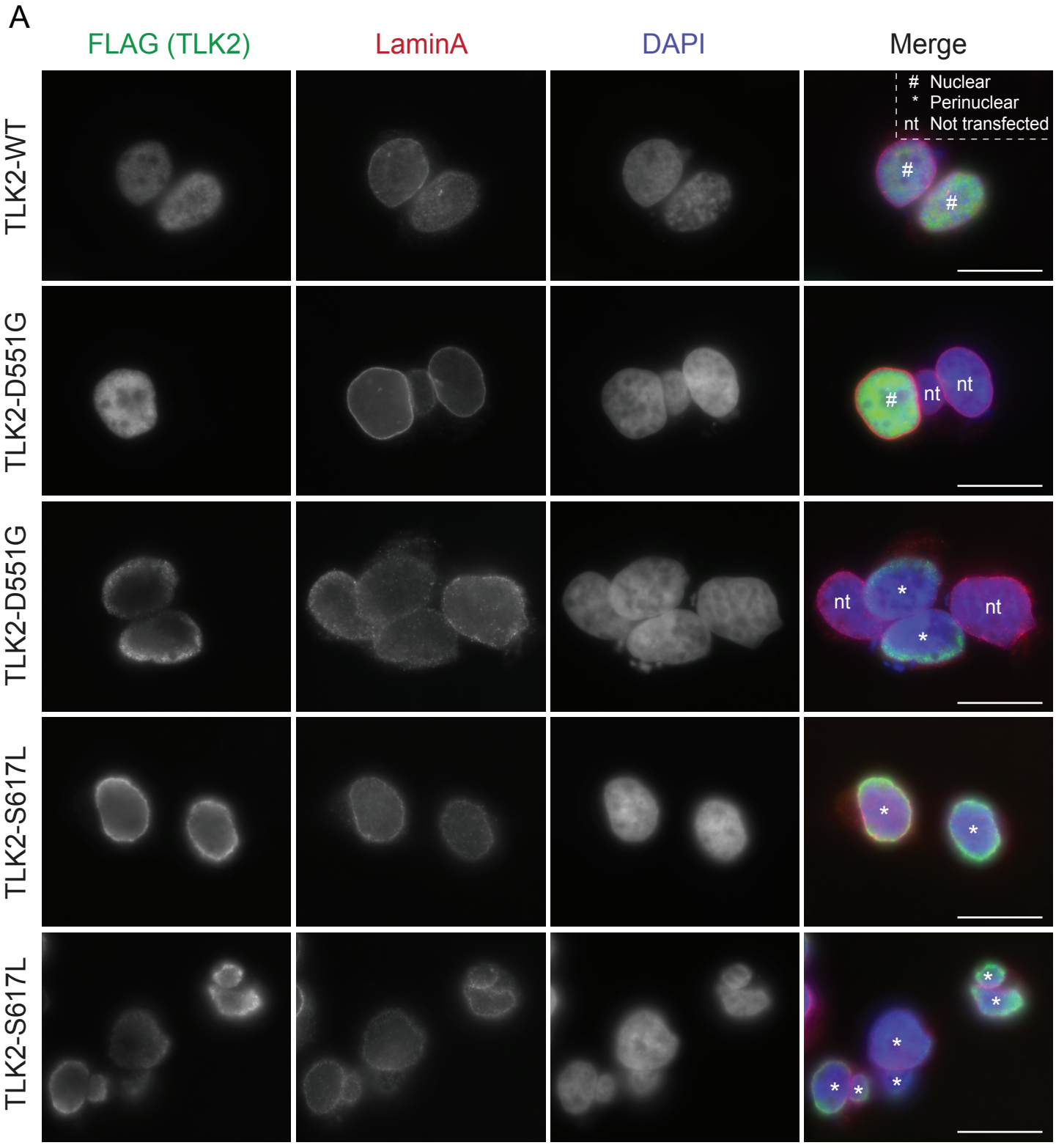
A
FLAG (TLK2)
LaminA
DAPI
Merge
Nuclear
* Perinuclear
nt Not transfected
TLK2-WT
TLK2-D551G
TLK2-D551G
TLK2-S617L
TLK2-S617L

Supplementary Figure 4

A Functionally studied missense variants

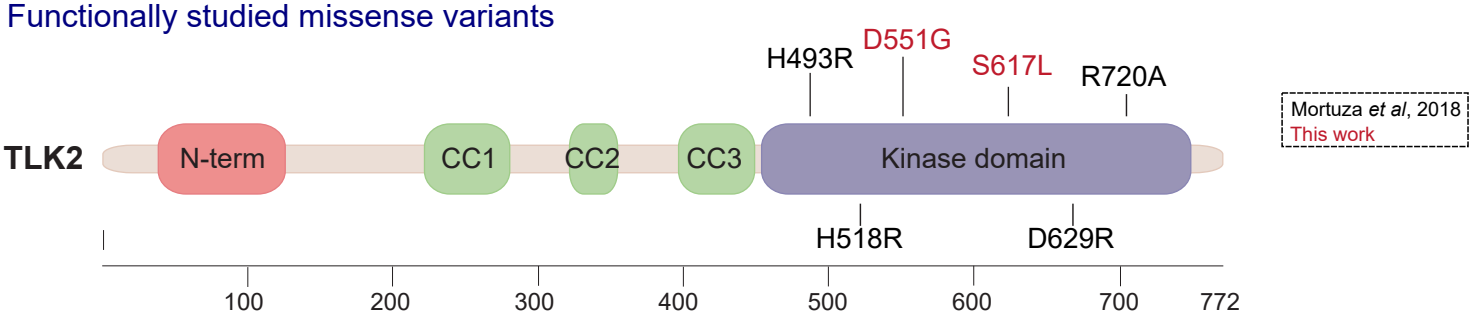

B

		ASF1A phosphorylation	TLK2 auto-phosphorylation	Effect on tridimensional structure	Localization	mRNA expression	Protein expression	Proximal interactome
Mortuza et al.; Nat Commun.; 2018	p.(His493Arg)	Less than 50%	Less than 50%	Catalytic site impairment	Not available	Not available	Not available	Not available
	p.(His518Arg)			Regulatory spine impairment				
	p.(Asp629Asn)			Alteration of the activation loop				
	p.(Arg720Ala)			Disruption of the interaction with other residues				
This work	p.(Asp551Gly)		Highly variable	Weaken hydrogen bonds with the subsequent helix	Partially altered	Decreased	Increased	Altered
	p.(Ser617Leu)		Less than 50%	Introduction of a hydrophobic residue in place the auto-phosphorylation site in the activation loop	Altered	Not available	Increased	Altered

All the observations are compared to the wt condition.

C

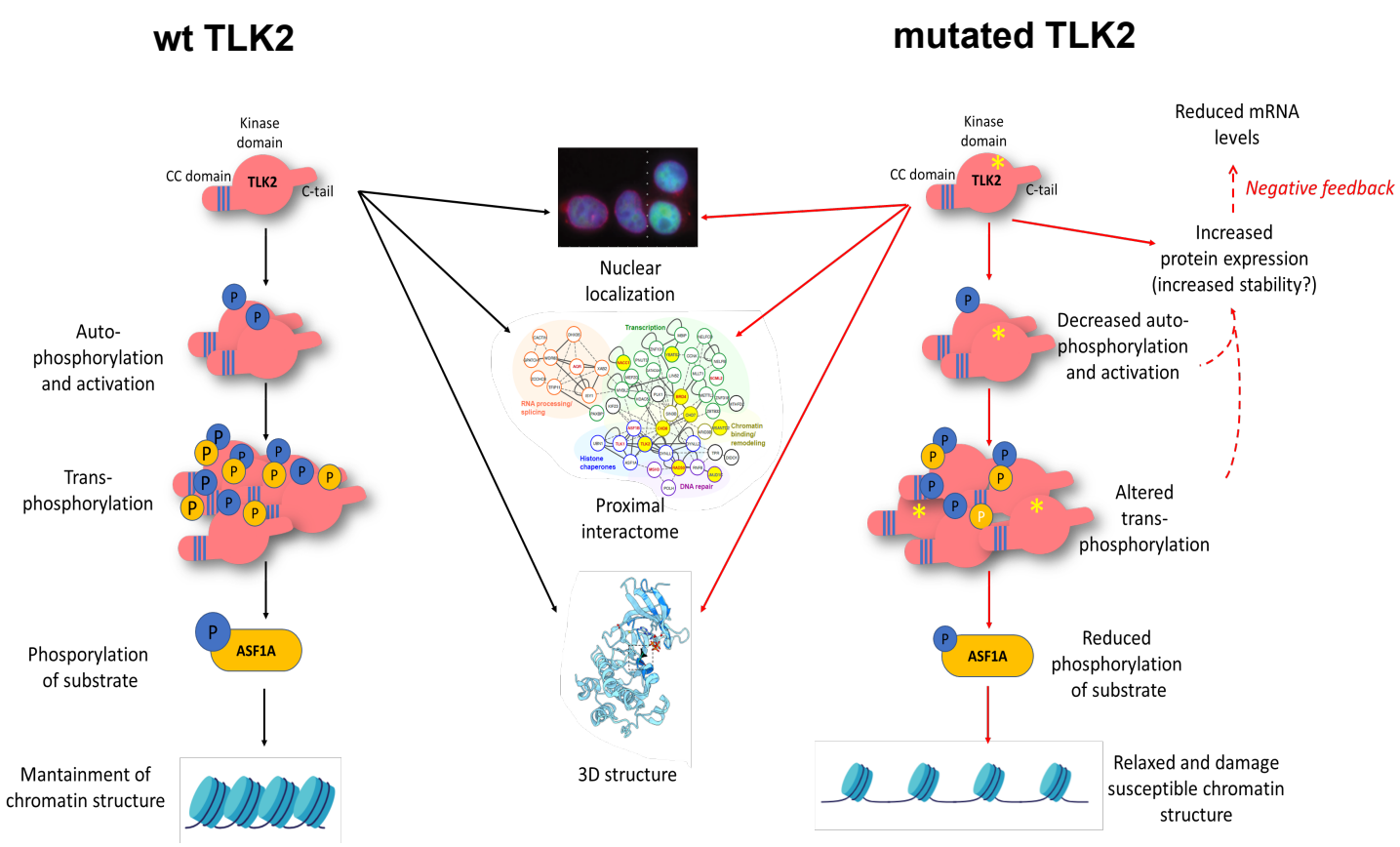

Functional analysis of *TLK2* variants and their proximal interactomes implicates impaired kinase activity and chromatin maintenance defects in their pathogenesis.

Lisa Pavinato [1], Marina Villamor-Payà [2], Maria Sanchiz-Calvo [2], Cristina Andreoli [3], Marina Gay [2], Marta Vilaseca [2], Gianluca Arauz-Garofalo [2], Andrea Ciolfi [4], Alessandro Bruselles [5], Tommaso Pippucci [6], Valentina Prota [3], Diana Carli [7], Elisa Giorgio [1], Francesca Clementina Radio [4] Vincenzo Antona [8], Mario Giuffrè [8], Kara Ranguin [9], Cindy Colson [9], Silvia De Rubeis [10, 11, 12, 13], Paola Dimartino [14], Joseph Buxbaum [10, 11, 12, 13, 15, 16], Giovanni Battista Ferrero [7], Marco Tartaglia [4], Simone Martinelli [5], Travis H. Stracker [*2], Alfredo Brusco [*1, 17, 18]

SUPPLEMENTARY MATERIAL AND METHODS

Whole exome sequencing, prioritization, and variant calling

Whole Exome Sequencing (WES) data processing, variant filtering, and prioritization by allele frequency, predicted functional impact, and inheritance models were performed using an in-house implemented pipeline, which mainly takes advantage of the Genome Analysis Toolkit (GATK v.3.7). High-quality variants with an effect on the coding sequence or affecting splice site regions were filtered against public databases (dbSNP150 and GnomAD V.2.1) to retain: i) private and clinically associated variants; ii) annotated variants with an unknown frequency or having MAF <0.1%. The functional impact of variants was analyzed by Combined Annotation Dependent Depletion V.1.3 and using ACMG/AMP 2015 guidelines.

Identified variants were confirmed by Sanger sequencing using standard conditions; primer sequences are listed in table S1.

Variants have been deposited on ClinVar database with submission ID SUB8204586 (p.Asp551Gly), SUB8204660 (p.Glu475Ter), SUB8209291 (p.Ser617Leu) and SUB8204671 ((17)(q23.2)del).

Briefly, gDNA extracted from whole blood was amplified with touchdown PCR (annealing temperature 65-58°C) using KAPA2G Fast HotStart Taq (Merck). PCR products were further purified with FastAP Thermosensitive Alkaline Phosphatase following manufacturer instructions and subjected to Sanger sequencing, using BigDye™ Terminator v3.1 Cycle Sequencing Kit (both from ThermoFisher Scientific).

Table S1. Primers and probes used in Sanger sequencing/ RT-PCR.

Variant/assay	Forward primer	Reverse primer	Note
c.1652A>G	5'-aaaggagtgagaagctgatgacc	5'-caaagaaaacccactaatactgtctcc	
c.1423G>T	5'-agaccagcacccaagtcc	5'-tgtattctgcttggtcacttagg	
TLK2-expression assays	5'-ggcactcctaggggacataa	5'-caactggtggaacacttctgc	UPL probe #72
	5'-cattccttatccaatcccttacc	5'-gacatgagggttggcagag	UPL probe #68

Table S2. Comparison between transcript NM_001284333.2 and NM_006852.6

NM_001284333.2 (Q86UE8-1; isoform 1)	**NM_006852.6 (Q86UE8-2; isoform 2)**

c.163A>G	(p.Lys55Glu)	c.163A>G	(p.Lys55Glu)
c.1423G>T	(p.Glu475Ter)	c.1357G>T	(p.Glu453Ter)
c.1652A>G	(p.Asp551Gly)	c.1586A>G	(p.Asp529Gly)
c.1850C>T;	p.(Ser617Leu)	c.1784C>T	(p.Ser595Leu)

p.(Asp551Gly) cDNA and splicing analysis

To analyse the effect of p.(Asp551Gly) variant on complementary DNA (cDNA), we designed a primer pair encompassing exons from 18 to 23 (forward primer: 5'- GCATGCATGTAGGGAATACCG; reverse primer: 5'-TGAACAGTTTGTGGCCTTGG). cDNA derived from both WT and mutated lymphoblastoid cell lines (LCLs) was amplified as described above with touchdown PCR (annealing temperature 65-58°C) and subsequently subjected to Sanger sequencing as described in previous paragraph.

To analyse the effect of the variant on splicing, 2 µl of PCR products were loaded in 1% Agarose gel (1X Tris-Borate-EDTA Buffer, 2% agarose, 0,1% EuroSafe Nucleic Acid Stain). A homemade loading dye (sucrose 44% and 2,5% bromophenol blue, ratio 16:1) was used; base pair were detected comparing to O'GeneRuler 1 kb (ThermoFisher Scientific). Gel was run for 30 minutes and band size was observed, acquiring images under UV light using ChemiDoc Imaging System (BioRad).

TLK2 protein expression

Total proteins were extracted from cellular pellet with RIPA buffer (50mM Tris-HCl pH 7.5; 150 mM NaCl; 1% NP-40; 0.5% Sodium Deoxycholate) supplemented with DTT 0.1 M, EDTA 0.5 M and 100x Halt Protease and Phosphatase Inhibitor Cocktail (Thermo Fisher Scientific). Fifteen micrograms of proteins were diluted into 4X LDS sample buffer and 10X Sample Reducing Agent and were electrophoresed on 4–12% Bis-Tris Protein Gels (Thermo Fisher Scientific).

Nitrocellulose membranes (0.45 µm pore, Biorad) were reversible stained with MemCode™ Reversible Protein Stain Kit (Thermo Fisher Scientific) and immunoblotted with the antibodies as indicated in Table S4. Images were acquired with ChemiDoc Imaging System and analysed with ImageLab software (BioRad), using volume tools quantification with global subtraction method. Statistical analysis was performed using two-tailed unpaired Student's t test with Welch's correction.

Single-cell gel electrophoresis

A LCLs harbouring the p.(Asp551Gly) variant, fibroblasts carrying the 39-kb deletion encompassing *TLK2*, and their wild-type counterparts were suspended in 0.7% low-melting agarose. Slides were prepared in duplicates with control cells and cells from affected subjects placed at the opposite sides of the same slide, and kept overnight in lysis solution at 4°C. Following lysis, slides were moved to alkaline buffer (20 min) to unwind DNA. Electrophoresis was performed for 20 or 60 minutes at 20 V, 300 mA (0.8 V/cm), at 4°C. Slides were then neutralized in 0.4 M Tris pH 7.5 (3x5 minutes), treated with absolute ethanol, stained with GelRed (Biotium), and analysed at a fluorescence microscope (Leica). Tail moments values were calculated by using a dedicated image analysis system (IAS2000 Delta Sistemi, Italy). To measure the extent of DNA damage induced by γ-ray irradiation and repair capability, LCLs were irradiated with 2-Gy or 4-Gy γ-rays from a ^{137}Cs source (0.8 Gy/min). During the treatment, cells were kept on ice to prevent DNA repair. Repair kinetics were assessed by SCGE as described above. Residual DNA damage was evaluated after 15 and 30 minutes at 37°C. For each experimental point, at least 100 nucleoids were analysed. Statistical analysis was performed using two-tailed unpaired Student's t test.

In silico modeling of TLK2 mutations

TLK2 mutations were modelled using the crystal structure of the TLK2 PKD (pdb: 5O0Y, https://www.wwpdb.org/pdb?id=pdb_00005o0y)[1] and the Structuropedia web interface (http://mod.farooq.ac/) for Modeller (https://salilab.org/modeller/)[2].

Site-directed mutagenesis

TLK2 mutations were generated using the QuickChange Lightning site-directed mutagenesis kit (Agilent Technologies) on the plasmids pcDNA3.1 N-SF-TAP-TLK2-WT[1] and BirA*-N-term-TLK2-WT[3] following manufacturer's instructions. Primers used are indicated in table S3. All constructs were sequenced (Macrogen) with the primer 5'-CTTTTCACTGGATACTGAC. Constructs were subsequently transfected in AD-293 cells.

Table S3. Site-directed mutagenesis primers.

Mutant	Primer	Sequence 5'-3'
TLK2-D551G (c.1652A>G; p.(Asp551Gly))	Fw	5'-TTTCAGGTAGAAGTCCAGACCATTTCCCTCACAGTATTC
	Rv	5'-GAATACTGTGAGGGAAATGGTCTGGACTTCTACCTGAAA
TLK2- S617L (c.1850C>T; p.(Ser617Leu))	Fw	5'-CTATCATCATCCATGATCTTCAAAAGACCAAAATCTGTAATTTTTATCTC
	Rv	5'-GAGATAAAAATTACAGATTTTGGTCTTTTGAAGATCATGGATGATGATAG

Transfection and affinity purification in mammalian cells

AD-293 cells were seeded in 15 cm plates and transiently transfected the next day with 20 ug of plasmid DNA using polyethylenimine (PEI) (Polysciences Inc., Warrington, PA) and 150mM NaCl. Medium was changed 6-8 hours post-transfection. Cells were harvested 48 hours post-transfection and collected by scraping in PBS. Pelleted cells were lysed in 1 mL of ice-cold lysis buffer (50 mM Tris-HCl pH 7.5, 150mM NaCl, 1% Tween-20, 0.5% NP-40, 1X protease inhibitor cocktail (Roche) and 1X phosphatase inhibitor cocktails 2&3 (Sigma-Aldrich)) on ice for 20 min. Cells were sonicated at medium intensity for 15 mins (Bioruptor XL; Diagenode), and lysates were cleared by centrifugation at 16000g for 20 mins at 4ºC. 100 µL of the lysate were retained for inputs. 4 mg of the total protein extracts were incubated with 100 µL of pre-washed Strep-Tactin superflow resin (IBA GmbH, Gottingen, Germany) overnight at 4ºC using an overhead tumbler. The resin was washed 3 times with 500 µL wash buffer (30 mM Tris-HCl pH 7.4, 150 mM NaCl, 0.1% NP-40, 1X protease inhibitor cocktail (Roche) and 1X phosphatase inhibitor cocktails 2&3 (Sigma-Aldrich)). The proteins were eluted from the Strep-Tactin matrix in 50 µL of elution buffer (5x desthiobiotin elution buffer (IBA GmbH) in TBS buffer (30 mM Tris-HCl pH 7.4, 150 mM NaCl, 0.1% NP-40, 1X protease inhibitor cocktail (Roche) and 1X phosphatase inhibitor cocktails 2&3 (Sigma-Aldrich)) for 10 mins on ice.

Table S4. Antibodies used in this study.

Antigen	Species	Source & reference	Dilution

TLK1	Rabbit	Cell Signaling #4125	1:1000 (WB)
TLK2	Rabbit	Bethyl Laboratories A301-257A	1:1000 (WB)
ASF1A	Rabbit	Groth Laboratory[4]	1:2000 (WB)
LC8	Rabbit	Abcam ab51603, clone EP1660Y	1:1000 (WB)
CHD7	Rabbit	Bethyl Laboratories A301-223A	1:2000 (WB)
CHD8	Rabbit	Bethyl Laboratories A301-224A	1:2000 (WB)
FLAG	Mouse	Sigma-Aldrich F3165, clone M2	1:5000 (WB)
VINCULIN	Rabbit	Millipore, #AB6039	1:5000 (WB)
Strep-tag	Mouse	IBA GmbH 2-1509-001	1:1000 (WB)
M2 Flag	Mouse	Sigma-Aldrich F1804	1:500 (IF)
LaminA	Rabbit	SC-20680	1:500 (IF)
Protein A/G	anti-Rabbit HRP	Thermo Fisher Scientific 32490	1:15000 (WB Nitro) 1:30000 (WB PVDF)
Mouse IgG	goat anti-mouse HRP	Thermo Fisher Scientific 31430	1:15000 (WB Nitro) 1:30000 (WB PVDF)
Alexa Fluor 488	Goat anti-mouse IgG	Thermo Fisher Scientific A28175	1:500 (IF)
Alexa Fluor 594	Goat anti-rabbit IgG	Thermo Fisher Scientific A11012	1:500 (IF)

***In vitro* kinase assays from cell lysates**

In vitro kinase assays were performed as previously described with minor modifications. after Strep-AP of pcDNA3.1 N-SF-TAP TLK2 from AD-293 cells. 200 µg of Strep-AP were incubated with 2 µCi ^{32}P-γ-ATP, 100 µM cold ATP, 1 µg of purified GST-ASF1A protein (kind gift from Anja Groth[5]) in 12 µL of kinase buffer (50mM Tris-HCl pH 7.5, 10 mM $MgCl_2$, 2mM DTT, 1X protein inhibitor cocktail (Roche) and 1X phosphatase inhibitor cocktails 2&3 (Sigma-Aldrich)). The reaction was incubated at 30ºC for 30 min. After that, the reaction was stopped by adding 4 µL of Sample Buffer (6x SDS, (0.2% bromophenol blue and *β*-mercaptoethanol), and boiled for 5-10 mins at 95ºC. Samples were analyzed on SDS-PAGE, stained with Coomassie Blue for 1 hour, washed 4 times with destaining buffer (10% acetic acid, 40% methanol, and 50% H_2O) and vacuum dried with an SGD2000 (Savant) for 2 hours at 60ºC. TLK2 and ASF1A phosphorylation

were measured using a Typhoon 8600 Variable Mode Imager (Molecular Dynamics) and band intensity quantified using ImageJ[6].

Immunofluorescence

AD-293 cells were seeded and transiently transfected with the indicated plasmids. The next day, cells were trypsinized and seeded on poly-L-Lysine-coated coverslips. 48 hours post-transfection, cells were fixed with 4% formaldehyde (Santa Cruz Biotechnology) for 10 mins and permeabilized in 0.2% Triton X-100 (Sigma-Aldrich) in 1x PBS for 10 mins at room temperature (R/T). Coverslips were washed twice with PBS and blocked with PBS-BT (0.1% Triton X-100, 3% BSA (Sigma-Aldrich) in PBS) for 30 min at R/T. The coverslips were incubated with the corresponding primary antibodies (Table S4) for 4 hrs at 4ºC in a humid chamber. After three washes with PBS-BT, the coverslips were incubated with the secondary antibody (Table S4) for 1 hour at R/T in a dark humid chamber. The coverslips were washed 3 times in PBS-BT and 4′,6-diamidino-2-phenylindole (DAPI) was added diluted 1:3000 in the first wash. Fluorescent images were acquired with an Orca AG camera (Hamamatsu) mounted on a Leica DMI6000B microscope equipped with 1.4 numerical aperture 100X oil immersion objective. The phenotypic distribution was quantified in 10 different fields of view in each condition.

Proximity-dependent biotin identification mass spectrometry (BioID-MS)

AD-293 cells were seeded in 15 cm plates and transiently transfected the next day with 20 µg of BirA* plasmids using PEI and 150 mM NaCl as described. Medium was changed 6-8 hours post-transfection. 24 hours post-transfection, 50 µM of biotin (IBIAN Biotechnology; 2-1016-002) were added per plate. For mass spectrometry, 5x15cm plates were used per condition. 48 hours post-transfection, the cells were harvested with Trypsin-EDTA (Sigma-Aldrich) and the 5 plates per condition were pooled together. Cell pellets were washed twice in cold PBS and lysed in 5 mL of cold lysis buffer (50 mM Tris-HCl pH 8.0, 150 mM NaCl, 0.1% SDS, 2 mM Mg_2Cl, 1% Triton X-100 (Sigma-Aldrich), 1mM EDTA (Sigma-Aldrich), 1mM EGTA (Sigma-Aldrich), 1:2000 benzonase 25 U/mL (Sigma-Aldrich), 1x protease inhibitor cocktail (Roche) and 1x phosphatase inhibitor cocktails 2&3 (Sigma-Aldrich)). 100 µL of the lysate were retained for Western blotting analysis. The remaining lysate was incubated with streptavidin-sepharose beads (GE Healthcare 2-1206-010)

during 3 hours in an end-over-end rotator at 4ºC in order to isolate the biotinylated proteins. The beads were washed once in lysis buffer and three times in 50 nM ammonium bicarbonate pH 8.3 buffer. Samples were snap-frozen and sent to the Mass Spectrometry & Proteomics Core Facility at IRB Barcelona for tryptic digestion and analysis.

Tryptic digestion was performed directly on beads by incubation with 2 ug of trypsin in 50 mM NH_4HCO_3 at 37ºC overnight. The next morning, an additional 1 µg of trypsin was added and incubated for 2 h at 37°C. The digestion was stopped by adding formic acid to 1% final concentration. Samples were cleaned through C18 tips (polyLC C18 tips) and peptides were eluted with 80% acetonitrile, 1% TFA. Samples were diluted to 20% acetonitrile, 0.25% TFA, loaded into strong cation exchange columns (SCX) and peptides were eluted in 5% NH_4OH, 30% methanol. Finally, samples were evaporated to dry, reconstituted in 50 µL and diluted 1:8 with 3% acetonitrile, 1% formic acid aqueous solution for nanoLC-MS/MS analysis.

The nano-LC-MS/MS was set up as follows. Digested peptides were diluted in 3% ACN/1% FA. Sample was loaded to a 300 µm × 5 mm PepMap100, 5 µm, 100 Å, C18 µ-precolumn (Thermo Scientific) at a flow rate of 15 µl/min using a Thermo Scientific Dionex Ultimate 3000 chromatographic system (Thermo Scientific). Peptides were separated using a C18 analytical column Acclaim PEPMAP 100 75 µm x50 cm nanoviper C18 3 µm 100A (Thermo Scientific) with a 90 min run, comprising three consecutive steps with linear gradients from 3 to 35% B in 60 min, from 35 to 50% B in 5 min, and from 50% to 85% B in 2 min, followed by isocratic elution at 85% B in 5 min and stabilization to initial conditions (A= 0.1% FA in water, B= 0.1% FA in CH_3CN). The column outlet was directly connected to an Advion TriVersa NanoMate (Advion) fitted on an Orbitrap Fusion Lumos™ Tribrid (Thermo Scientific). The mass spectrometer was operated in a data-dependent acquisition (DDA) mode. Survey MS scans were acquired in the Orbitrap with the resolution (defined at 200 m/z) set to 120,000. The lock mass was user-defined at 445.12 m/z in each Orbitrap scan. The top speed (most intense) ions per scan were fragmented by CID and detected in the linear ion trap. The ion count target value was 400,000 and 10,000 for the survey scan and for the MS/MS scan respectively. Target ions already selected for MS/MS were dynamically excluded for 15s. Spray voltage in the NanoMate source was set to 1.60 kV. RF Lens were tuned to 30%. Minimal signal required to trigger MS to MS/MS switch was set to 5,000. The

spectrometer was working in positive polarity mode and singly charge state precursors were rejected for fragmentation.

We performed a twin database search with two different softwares, Thermo Proteome Discoverer v2.3.0.480 (PD) and MaxQuant v1.6.6.0 (MQ). The search engine nodes used were Sequest HT for PD and Andromeda for MQ. The databases used in the search was SwissProt Human (release 2019 01) including contaminants and TLK1 and TLK2 proteins. We run the search against targeted and decoy databases to determine the false discovery rate (FDR). Search parameters included trypsin enzyme specificity, allowing for two missed cleavage sites, oxidation in M and acetylation in protein N-terminus as dynamic modifications. Peptide mass tolerance was 10 ppm and the MS/MS tolerance was 0.6 Da. Peptide were filtered at a false discovery rate (FDR) of 1 % based on the number of hits against the reversed sequence database.

For the quantitative analysis, contaminant identifications were removed and unique peptides (peptides that are not shared between different protein groups) were used for the quantitative analysis with SAINTexpress-spc v3.6.1[7]. SAINTexpress compares the prey control spectral counts with the prey test spectral counts for all available replicates. For each available bait and for each available replicate, we took as prey count the maximum count result between PD and MQ. Once obtained this combined dataset, we ran the SAINTexpress algorithm with TLK2 samples and a number of controls samples from previous experiments in the same cell type (n=45 total). High confidence interactors were defined as those with a SAINT score of 0.7 or greater. Output data from SAINTexpress is available upon request and raw data is available in the PRIDE repository, accession number PXD019450.

Table S5. In silico predictors for p.(Asp551Gly) and p.(Ser617Leu) variants

Tool	Predicted impact	
	p.(Asp551Gly)	**p.(Ser617Leu)**
BayesDel addAF *dbNSFP version 4.1*	Damaging	Damaging
BayesDel noAF *dbNSFP version 4.1*	Damaging	Damaging
DEOGEN2 *dbNSFP version 4.1*	Tolerated	Tolerated
EIGEN *dbNSFP version 4.1*	Pathogenic	Pathogenic
EIGEN PC *dbNSFP version 4.1*	Pathogenic	Pathogenic
FATHMM *dbNSFP version 4.1*	Tolerated	Tolerated
FATHMM-MKL *dbNSFP version 4.1*	Damaging	Damaging
FATHMM-XF *dbNSFP version 4.1*	Damaging	Damaging
LIST-S2 *dbNSFP version 4.1*	Damaging	Damaging
LRT *dbNSFP version 4.1*	Deleterious	Deleterious
MetaLR *dbNSFP version 4.1*	Tolerated	Damaging

MetaSVM *dbNSFP version 4.1*	Tolerated	Damaging
MutPred *dbNSFP version 4.1*	Pathogenic	Pathogenic
Mutation assessor *dbNSFP version 4.1*	Medium	Medium
MutationTaster *dbNSFP version 4.1*	Disease causing	Disease causing
MVP *dbNSFP version 4.1*	Pathogenic	Tolerated
PROVEAN *dbNSFP version 4.1*	Damaging	Damaging
PrimateAI *dbNSFP version 4.1*	Damaging	Damaging
REVEL *dbNSFP version 4.1*	Pathogenic	Pathogenic
SIFT *dbNSFP version 4.1*	Damaging	Damaging
SIFT4G *dbNSFP version 4.1*	Damaging	Damaging

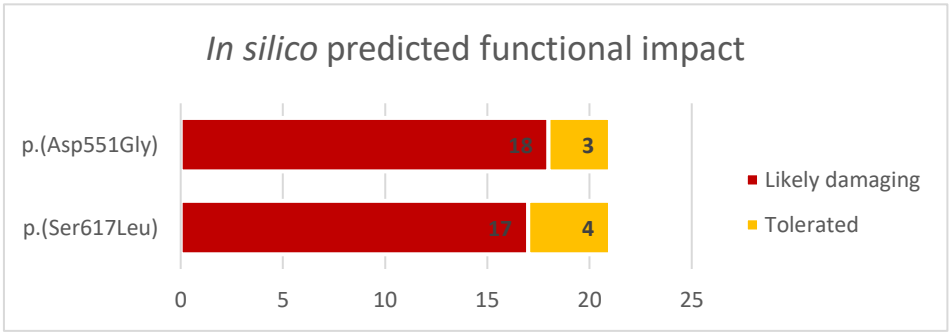

Table S6. Clinical characterization of patients carrying TLK2 variants

	Case 1	**Case 2**	**Case 3**	**Case 4**	**Case 5**	**Case 6**
	c.1652A>G; p.(Asp551Gly)	**(c.1423G>T; p.(Glu475Ter))**	**(c.1423G>T; p.(Glu475Ter))**	**(c.1423G>T; p.(Glu475Ter))**	**(c.1423G>T; p.(Glu475Ter))**	**del17q23.2**
Sex	Male	Female	Female	Male	Male	Female
Age at last examination	11	47	26	16	3	16
Ethnicity	Caucasian	Caucasian	Caucasian	Caucasian	Caucasian	Caucasian
ASD	+	-	-	-	-	-
ID	+	+	+	+	N.A.	N.A.
IQ≤70	-	-	+	+	-	-
IQ 71-85	+	+	-	-	-	-
IQ 86-100	-	-	-	-	-	-
Social-emotional problems	+	-	+	+	-	-
Tantrums	-	-	-	-	-	-
ADHD	+	-	+	+	+	-
Brain abnormality	-	-	-	-	+	-
Hypotonia	-	-	-	+	+	-
Speech delay	+	-	+	+	+	-
Bipolar disorder	-	-	-	-	-	-
Epilepsy	-	-	-	-	-	-
Obsessive compulsive behaviour	+	-	+	-	-	-
Anxiety	+	-	+	+	-	-
Aggressiveness	-	-	+	+	-	-
Difficulties in memory and transcription	-	-	+	+	-	+
Difficulties in reading and writing	+	-	+	+	-	-
Short attention span	+	-	+	-	-	-
Delayed motor development	+	-	-	-	-	+
Microcephaly	-	+	+	+	+	-
Gastrointestinal problems	-	-	-	-	-	-
Plagiocephaly	-	-	+	+	+	-
Skeletal anomalies of the hands	+	-	-	-	-	+
Skeletal anomalies of the feet	-	-	+	+	-	-
Joint hypermobility	+	-	+	+	-	-

Other minor skeletal anomalies	-	-	+	+	-	-
Dysmorphic facial features	+	+	+	+	+	+

+ = observed; -= not observed; N.A.= not available

SUPPLEMENTAL NOTE: CASE REPORTS

Family 1 – Case 1

The patient was the only child of healthy unrelated Caucasian parents. The mother presented one spontaneous miscarriage of the first trimester and one pregnancy ended with intrauterine death at 21 weeks of gestation for severe cardiomyopathy. The maternal uncle presented schizophrenia and the maternal aunt presented depression. Remaining family history is unremarkable.

Pregnancy, physiologically conceived, started bigeminal and was complicated by loss of the twin at 9 weeks of gestation, threat of abortion at the 4th and 5th month, oligoamnios and decreased fetal movements.

He was born at 41+0 weeks of gestation by spontaneous delivery with weight 2850 gr (5° centile, -0.68 SD), length 48.7 cm (10° centile, -1.3 SD), OFC 33.9 cm (20° centile, -0.84 SD). APGAR score was 8 and 9 at 1st and 5th minute, respectively.

Slight feeding difficulties with poor growth have been reported in the first months of life.

He presented mild motor delay with sitting at 9 months of age and walking at 20 months of age and language delay with first words at 12 months and first sentences at 3 years.

He presented tendency to isolation and was diagnosed with autism at 6.5 years.

He presented pavor nocturnus until 7 years of age, short attention span, good memory, anxiety, compulsive obsessive behavior and difficulties in writing.

EEG, brain MRI and abdominal ultrasound at 5 years of age were normal. IQ evaluation with WISC-III scale showed a total IQ of 83 (borderline).

At last physical examination at 11 years of age he presented height 143 cm (32° centile, -0.46 SD), weight 43 kg (67° centile, +0.43 SD), OFC 54 cm (64° centile, +0.35 SD). The calculated body mass index (BMI) was in the range of normal (BMI 21).

Dysmorphic features included upslanting palpebral fissures, prominent nasal bridge, broad nasal tip, low hanging columella, thin lips, prognatism, pointed chin. He also presented tapered fingers and mild joint hypermobility.

Family 2– Cases 2-5

The patients came from a non-consanguineous Italian family and came to attention thanks to genetic investigations required for affected patients 3 and 4, while patient 5 born meanwhile.

The mother (case 2) familial history was unremarkable. Her brother, her two sisters and her parents were never suspected of having intellectual disability, although detailed clinical information about them were not available. She had mild intellectual disability, that came to light only after a retrospective clinical evaluation after the identification of *TLK2* c.1423G>T; p.(Glu475Ter) variant by trio whole exome sequencing.

At last physical examination at 46 years of age she presented height 155 cm (10° centile, -1.27 SD), weight 68 kg (74° centile, +0.64 SD), OFC 52 cm (1° centile, -2.5 SD). She was overweight (BMI 28.3).

Dysmorphic features included lateral thin eyebrows, hypertelorism, upslanting palpebral fissures, prominent columella, broad nasal bridge and tip, short philtrum, thin upper lip, downturned corners of mouth, mandibular prognatism.

Patient 3 was the first female child, characterised by intellectual disability (IQ<70) and other behavioural and neurological issues, including social-emotional problems, attention deficit hyperactivity disorder, aggressiveness, anxiety, obsessive compulsive disorder and speech delay. She showed also difficulties in memory, transcription, reading and writing and a short attention span.

At last physical examination at 25 years of age she presented height 154 cm (8° centile, -1.43 SD), weight 70 kg (78° centile, +0.77 SD), OFC 52.5 cm (4° centile, -1.7 SD). She was overweight (BMI 29.5).

She presented strabismus, joint hypermobility, scoliosis, plagiocephaly and postaxial polydactyly of left foot.

Dysmorphic features included lateral thin eyebrows, hypertelorism, upslanting palpebral fissures, prominent columella, broad nasal tip, macrostomia, thin upper lip, downturned corners of mouth, mandibular prognatism.

Patient 4 has been subjected to whole exome sequencing as his older sister. He was characterized by intellectual disability (IQ<70), social-emotional problems, attention deficit hyperactivity disorder, anxiety and aggressiveness. Moreover, a speech delay and generalized hypotonia were observed. He had difficulties in memory, transcription, reading and writing.

At last physical examination at 15 years of age he presented height 185 cm (91° centile, +1.33 SD), weight 75 kg (91° centile, +1.33 SD), OFC 52 cm (3° centile, -1.95 SD). His BMI was in the range of normal (BMI 21.9).

As additional features, he was characterized by plagiocephaly, joint hypermobility, pes planus and strabismus. Overriding second toe was observed.

Dysmorphic features included telecanthus, prognatism, upslanting palpebral fissures, epicanthal folds, posteriorly rotated ears, low-implant auricles, synophrys, prominent columella, broad nasal tip, thick filter, long face, ptosis, thin upper lip and downturned corners of mouth.

Patient 5 was the last born of the family and *TLK2* c.1423G>T; p.(Glu475Ter) variant was detected after target Sanger sequencing following diagnosis of patient 3 and 4. He was too young to assess intellectual disability but he presented a global psychomotor delay, speech delay, hypotonia and attention deficit hyperactivity disorder.

At last physical examination at 2 years of age he presented height 80 cm (2° centile, -2.06 SD), weight 8,2 kg (<1° centile, -3.67 SD), OFC 43 cm (<1° centile, -3.96 SD), presenting an underweight situation (BMI 12.8).

He showed plagiocephaly and conductive hearing loss and brain MRI showed a mild hypoplasia of the corpus callosum.

His facial features were similar to the ones observed for the other affected relatives, including long face, prominent nasal bridge and broad nasal tip, thin vermilion of the upper lip, upslanting palpebral fissures, lateral thin eyebrows, downturned corners of mouth and high palate.

Family 3– Case 6

The 17-year-old Caucasian patient has a history of intellectual deficiency with thumb anomalies. She was born at 35 weeks by spontaneous vaginal birth with a weight of 2320g (2° centile, -2.10 SD), height 43.5cm (<1° centile, -2.67 SD), OFC 32.5cm (6° centile, -1.56 SD), with absence of flexure fold of the thumbs.

A persistent arterial canal was found and cured surgically. Feeding difficulties were present in the early age. She walked at 14 months. At 5 years of age, the patient weighted 13kg (1° centile, -2.54 SD) for a height of 96 cm (1° centile, -2.55 SD), OFC 48.5 cm (10° centile, -1.3 SD). Her BMI brought out an underweight (BMI 14.1); at 7 years, she was treated by growth hormone.

Dysmorphic characteristics included slightly short forehead, hypertelorism, a large nose root with epicanthi, bifid nasal tip. There was an absence of earlobes, the palpebral fissures were narrow and oriented upward. She had short hands with an impossibility of bending the thumbs, short and brittle nails. X rays of the thumbs were normal.

Academically, in 2nd grade school she was able to read and write. She had memory and transcription difficulties. She had no trouble concentrating. She benefited from treatment in speech therapy as well as physiotherapy and psychomotricity.

At 17 years of age, she weighed 43 kg (4° centile, -1.4 SD), height 155 cm (12° centile, -1.16 SD), OFC 53.8 cm (32° centile, -0.47 SD); as during the childhood, the patient maintained an underweight condition (BMI 17.9).

The tests performed for this patient included a chromosomal analysis and array-CGH. Array-CGH showed a *de novo* deletion in 17q23.2 with a size of 39-87 kb including *TLK2.*

Additional case (p.Ser617Leu)

Case carrying the de novo variant TLK2 c.1850C>T; p.(Ser617Leu) was a 12 years old non-hispanic white male. The proband received a clinical diagnosis (ADOS, Autism Diagnostic Observation Schedule) of autism spectrum disorder. He showed intellectual disability, with nonverbal IQ 74 and verbal IQ 63. Neither non-febrile nor febrile seizures were reported, as well as neurodevelopmental regression. The family was initially screened by array comparative genomic hybridization (aCGH) using a customized microarray[7] and no large

copy number variations were identified. Molecular diagnosis was reached by whole exome sequencing of the proband, an unaffected sibling and parents.

Table S7. Comparison between features observed in our cases and previously reported ones[8, 9]

Observed Features		Reijnders *et al.*	Töpf *et al.*	Our cases
Neurological and behavioural	Low normal ID (IQ 85-100)	72%	0%	0% (2/4)
	Borderline ID (IQ 70-85)	14%	0%.	50% (2/4)
	ID (IQ ≤70)	6%	100%	50% (2/4)
	Social-emotional problems	18%	n.r.	50% (3/6)
	Tantrums	32%	n.r.	0% (0/6)
	ASD	32%	n.r.	17% (1/6)
	ADHD/ADD	15%	n.r.	67% (4/6)
	Short attention span	5%	n.r.	33% (2/6)
	Anxiety	12%	n.r.	50% (3/6)
	Obsessive-compulsive behaviour	6%	n.r.	33% (2/6)
	Aggressiveness	6%	100%	33% (2/6)
	Difficulties in reading and writing	n.r.	n.r.	50% (3/6)
	Difficulties in memory and transcription	n.r.	n.r.	50% (3/6)
	Motor delay	89%	100%	33% (2/6)
	Language delay	92%	100%	67% (4/6)
	Pavor nocturnus	n.r.	n.r.	17% (1/6)
	Epilepsy	14%	100%	0% (0/6)
Growth parameters	Short stature	37%	n.r.	0% (0/6)
	Underweight	14%	n.r.	33% (2/6)
	Overweight	8%	n.r.	33% (2/6)

	Microcephaly	24%	100%	67% (4/6)
Gastro-intestinal problems	Constipation	60%	100%	0% (0/6)
	Diarrhoea	9%	n.r.	0% (0/6)
Skeletal	Scoliosis	9%	n.r.	17% (1/6)
	Contractures hands	9%	n.r.	0% (0/6)
	Postaxial foot polydactyly	n.r.	n.r.	17% (1/6)
	Overriding second toe	n.r.	n.r.	17% (1/6)
	Tapering fingers	n.r.	n.r.	17% (1/6)
	Short hands with short distal phalanx	n.r.	n.r.	17% (1/6)
Dysmorphic facial features	Abnormal palpebral fissures	55%	100%	100% (6/6)
	Prominent nasal bridge	68%	100%	67% (4/6)
	Broad nasal tip	66%	n.r.	83% (5/6)
	Bifid nasal tip	n.r.	n.r.	17% (1/6)
	Low hanging columella	n.r.	n.r.	33% (2/6)
	Thin lips	62%	100%	83% (5/6)
	Prognathism	n.r.	n.r.	83% (5/6)
	Pointed and tall chin	42%	n.r.	17% (1/6)
	Blepharophyimosis	82%	n.r.	0% (0/6)
	Telecanthus	n.r.	100%	33% (2/6)
	Epicanthal folds	42%	n.r.	33% (2/6)
	Narrow mouth	32%	n.r.	0% (0/6)
	High palate	30%	n.r.	50% (3/6)
	Microtia	29%	n.r.	0% (0/6)
	Posteriorly rotated ears	29%	n.r.	17% (1/6)
	Ears without lobes	n.r.	n.r.	17% (1/6)
	Low-implant auricle	n.r.	n.r.	17% (1/6)

	Long face	27%	n.r.	67% (4/6)
	Ptosis	21%	n.r.	17% (1/6)
	Wide spaced eyes/Hypertelorism	74%	n.r.	67% (4/6)
	Synophrys	n.r.	n.r.	17% (1/6)
	Macrostomia/Big mouth	n.r.	100%	17% (1/6)
	Downturned corners of mouth	n.r.	n.r.	67% (4/6)
Other features	Neonatal feeding difficulties	44%	100%	17% (1/6)
	Hypotonia	40%	100%	33% (2/6)
	Refraction abnormality	31%	n.r.	0% (0/6)
	Strabismus	29%	n.r.	33% (2/6)
	Recurrent otitis media	27%	n.r.	0% (0/6)
	Conductive hearing loss	16%	100%	17% (1/6)
	Joint hypermobility	24%	n.r.	50% (3/6)
	Pes Planus	25%	n.r.	17% (1/6)
	Plagiocephaly	16%	n.r.	50% (3/6)
	Hypertrichosis	17%	n.r.	0% (0/6)
	Brain abnormality	25%	100%	17% (1/6)
	Craniosynostosis	11%	n.r.	0% (0/6)
	Hoarse voice	9%	n.r.	0% (0/6)

n.r.= not reported; ID= intellectual disability; ASD= autism spectrum disorder; ADHD= attention deficit hyperactivity disorder; ADD= attention deficit disorder.

Features not previously reported in other cases are in bold.

Table S8. BioID-MS results. The first tab contains the unfiltered results for all baits. The second tab is the raw output of the SAINTexpress software (http://saint-apms.sourceforge.net/Main.html) and the third tab

contains the lists of proteins used for comparison to iPOND experiments or the SFARI (gene.sfari.org)/DECIPHER (decipher.sanger.ac.uk) databases.

Table S9. Classification of proximal interactors. The first tab is an alphabetical list of the proximal interactors identified for all baits. Their statistical significance is colour coded as in the legend and those found in the OMIM (omim.org) or SFARI (gene.sfari.org)/DECIPHER (decipher.sanger.ac.uk) databases are indicated. The second tab indicates only the SFARI genes identified with additional details about their molecular functions.

LEGENDS TO FIGURES.

Figure S1.

A) *TLK2* mRNA levels in fibroblasts from case 6 and in lymphoblastoid cell line derived from case 1. *TLK2* expression was significantly reduced both in LCL carrying p.(Asp551Gly) variant and in fibroblasts carrying the 17q23.2 deletion. All experiments were performed at least in triplicate. UPL probe #68 and primers indicated in Supplementary material and methods were used; *HMBS* and *GAPDH* mRNA expression was used as reference. Statistical analysis was performed using t-test with Welch's correction; ****= P value ≤ 0.0001. Numbers at the top of the bars indicated mean values. (B) Sanger sequencing of *TLK2* WT versus p.(Asp551Gly) variant. Results from sequencing of both gDNA and cDNA are showed, to allow a simply comparison. No differences in the peaks between p.(Asp551Gly) gDNA and cDNA were observed. (C) Splicing analysis of *TLK2* WT versus *TLK2* p.(Asp551Gly) variant. After 30 minutes of run on 1% agarose gel, LCLs from WT control and from patient showed the same base pair size. (D) Western Blot analysis showed a significantly increased TLK2 protein expression compared to controls (***p 0.0005; two-tailed unpaired Student's t test). TLK2 expression was normalized on Vinculin; MemCode image is reported as loading control.

Figure S2.

(A) SCGE assays documented that *TLK2* haploinsufficiency affects proper chromatin compaction. Fibroblasts carrying the 17q23.2 deletion encompassing TLK2 showed a more relaxed state of chromatin compared to control cells. Nucleoids of cells derived from subjects 6 showed a significantly higher tail moment value after 60 minutes of electrophoresis run time. For each point, at least 100 cells were analysed. Values are represented as mean ± SEM of three independent experiments.

Figure S3.

(A) Representative immunofluorescence microscopy of overexpressed TLK2-WT, TLK2-D551G, and TLK2-S617L in AD-293 cells. The different localization patterns are indicated as # for nuclear localization and * for perinuclear localization. Not transfected cells are indicated with nt. Scale bar = 20 μM.

Figure S4.

(A) Schematic representation of functionally studied missense variants. All the missense variants functionally studied are located in Kinase Domain (KD) as the majority of the other reported missense variants[8]. Already studied variants[1] are in black, while variants presented in this work are in red. (B) Summary of functionally tested variants reported in the work from Mortuza *et al.*[1] and the ones presented in this work. All the variants are able to alter ASF1A phosphorylation, causing at least a reduction of 50% compared to wt. Also TLK2 auto-phosphorylation was decreased for all the variants except for p.(Asp551Gly), for which the trend was not clear. Effect on tridimensional structure was predicted basing on the available TLK2 structure[1] and was altered by all variants analysed. Information about localization, expression and proximal interactome were not available for previous reported variants. (C) Schematic representation of the proposed working model. On the left, a brief description of TLK2 activity is proposed[1, 10]; on the right we represented the alteration we observed in cells harbouring missense variants both in this work and in previous[1]. We proposed a working model in which missense variants impair TLK2 auto-phosphorylation and ASF1A activation, leading to more relaxed chromatin state and increased susceptibility to DNA damage. At the same time, altered proteins seems to show an increased expression, probably reflecting a higher protein stability. We proposed that this increase in protein expression could be counterbalanced by a sort of negative feedback that cause the mRNA reduction we observed for p.(Asp551Gly) variant. Moreover, mutated proteins assume an altered intracellular localization and interplay with proximal interactors are impaired. *=mutation; CC=coiled-coil; P=phosphorylated; red arrows indicate impaired pathway, dotted red arrows indicate hypothesis not experimentally demonstrated.

REFERENCES

1 Mortuza GB, Hermida D, Pedersen AK, Segura-Bayona S, López-Méndez B, Redondo P, Rüther P, Pozdnyakova I, Garrote AM, Muñoz IG, Villamor-Payà M, Jauset C, Olsen J V., Stracker TH, Montoya G. Molecular basis of Tousled-Like Kinase 2 activation. *Nat Commun* Published Online First: 2018. doi:10.1038/s41467-018-04941-y

2 Webb B, Sali A. Comparative protein structure modeling using MODELLER. *Curr Protoc Bioinforma* Published Online First: 2016. doi:10.1002/cpbi.3

3 Segura-Bayona S, Knobel PA, Gonzalez-Buron H, Youssef SA, Peña-Blanco A, Coyaud E, Lopez-Rovira T, Rein K, Palenzuela L, Colombelli J, Forrow S, Raught B, Groth A, De Bruin A, Stracker TH. Differential requirements for Tousled-like kinases 1 and 2 in mammalian development. *Cell Death Differ* Published Online First: 2017. doi:10.1038/cdd.2017.108

4 Groth A, Ray-Gallet D, Quivy JP, Lukas J, Bartek J, Almouzni G. Human Asf1 regulates the flow of S phase histones during replicational stress. *Mol Cell* Published Online First: 2005. doi:10.1016/j.molcel.2004.12.018

5 Klimovskaia IM, Young C, Strømme CB, Menard P, Jasencakova Z, Mejlvang J, Ask K, Ploug M, Nielsen ML, Jensen ON, Groth A. Tousled-like kinases phosphorylate Asf1 to promote histone supply during DNA replication. *Nat Commun* Published Online First: 2014. doi:10.1038/ncomms4394

6 Schindelin J, Arganda-Carreras I, Frise E, Kaynig V, Longair M, Pietzsch T, Preibisch S, Rueden C, Saalfeld S, Schmid B, Tinevez JY, White DJ, Hartenstein V, Eliceiri K, Tomancak P, Cardona A. Fiji: An open-source platform for biological-image analysis. Nat. Methods. 2012. doi:10.1038/nmeth.2019

7 Teo G, Liu G, Zhang J, Nesvizhskii AI, Gingras AC, Choi H. SAINTexpress: Improvements and additional features in Significance Analysis of INTeractome software. *J Proteomics* Published Online First: 2014. doi:10.1016/j.jprot.2013.10.023

8 Reijnders MRF, Miller KA, Alvi M, Goos JAC, Lees MM, de Burca A, Henderson A, Kraus A, Mikat B, de Vries BBA, Isidor B, Kerr B, Marcelis C, Schluth-Bolard C, Deshpande C, Ruivenkamp CAL, Wieczorek D, Baralle D, Blair EM, Engels H, Lüdecke HJ, Eason J, Santen GWE, Clayton-Smith J, Chandler K, Tatton-Brown K, Payne K, Helbig K, Radtke K, Nugent KM, Cremer K, Strom TM, Bird LM, Sinnema M, Bitner-Glindzicz M, van Dooren MF, Alders M, Koopmans M, Brick L, Kozenko M, Harline ML, Klaassens M, Steinraths M, Cooper NS, Edery P, Yap P, Terhal PA, van der Spek PJ, Lakeman P, Taylor RL, Littlejohn RO, Pfundt R, Mercimek-Andrews S, Stegmann APA, Kant SG, McLean S, Joss S, Swagemakers SMA, Douzgou S, Wall SA, Küry S, Calpena E, Koelling N, McGowan SJ, Twigg SRF, Mathijssen IMJ, Nellaker C, Brunner HG, Wilkie AOM. De Novo and Inherited Loss-of-Function Variants in TLK2: Clinical and Genotype-Phenotype Evaluation of a Distinct Neurodevelopmental Disorder. *Am J Hum Genet* 2018;**102**:1195–203.

9 Töpf A, Oktay Y, Balaraju S, Yilmaz E, Sonmezler E, Yis U, Laurie S, Thompson R, Roos A,

MacArthur DG, Yaramis A, Güngör S, Lochmüller H, Hiz S, Horvath R. Severe neurodevelopmental disease caused by a homozygous TLK2 variant. *Eur J Hum Genet* Published Online First: 2019. doi:10.1038/s41431-019-0519-x

10 Segura-Bayona S, Stracker TH. The Tousled-like kinases regulate genome and epigenome stability: implications in development and disease. Cell. Mol. Life Sci. 2019. doi:10.1007/s00018-019-03208-z